AD

Technical Report ARAEW-TR-04003

PHYSICAL VAPOR DEPOSITION SIMULATIONS OF MICROSTRUCTURE EVOLUTION

Mark Johnson, Paul Cote

APRIL 2004

ARMAMENT RESEARCH, DEVELOPMENT AND ENGINEERING CENTER
Armaments Engineering & Technology Center
Weapon Systems & Technology
Benét Laboratories
Watervliet, New York

APPROVED FOR PUBLIC RELEASE; DISTRIBUTION UNLIMITED

REPORT DOCUMENTATION PAGE

Form Approved
OMB No. 0704-0188

1. REPORT DATE *(DD-MM-YYYY)*	2. REPORT TYPE	3. DATES COVERED *(From - To)*
April 2004	FINAL	

4. TITLE AND SUBTITLE
Physical Vapor Deposition Simulations of Microstructure Evolution

5a. CONTRACT NUMBER

5b. GRANT NUMBER

5c. PROGRAM ELEMENT NUMBER

6. AUTHOR(S)
Mark Johnson, Paul Cote

5d. PROJECT NUMBER

5e. TASK NUMBER

5f. WORK UNIT NUMBER

7. PERFORMING ORGANIZATION NAME(S) AND ADDRESS(ES)
U.S. Army ARDEC
Benet Laboratories, RDAR-WSB
Watervliet, NY 12189-4000

8. PERFORMING ORGANIZATION REPORT NUMBER
ARAEW-TR-04003

9. SPONSORING/MONITORING AGENCY NAME(S) AND ADDRESS(ES)
U.S. Army ARDEC
Benet Laboratories, RDAR-WSB
Watervliet, NY 12189-4000

10. SPONSOR/MONITOR'S ACRONYM(S)

11. SPONSORING/MONITORING AGENCY REPORT NUMBER

12. DISTRIBUTION AVAILABILITY STATEMENT
Approved for public release; distribution is unlimited.

13. SUPPLEMENTARY NOTES

14. ABSTRACT
Physical vapor deposition (PVD) is currently being explored as an alternative to electrodeposition for coating the bore of large caliber cannon. PVD is an efficient and environmentally friendly means of producing protective coatings. A number of experimental PVD systems have been developed using cylindrical magnetron sputtering (CMS) to provide a thick metal coating on the bore of cannon. However, adherent, erosion and corrosion resistant coatings are critical to the performance of many weapon systems and the process control parameters that produce the optimal coating properties have not yet been identified. A number of promising coatings have been produced, but a significant number of costly experiments are required before these parameters can be established. Therefore, there is a need for further guidance in selecting the experiments. A model capable of predicting important coating properties such as adhesion, cohesion, density, compositional variation, and uniformity is desirable, but currently not available.

15. SUBJECT TERMS
Physical vapor deposition (PVD); coatings; cylindrical magnetron sputtering (CMS)

16. SECURITY CLASSIFICATION OF:			17. LIMITATION OF ABSTRACT	18. NUMBER OF PAGES	19a. NAME OF RESPONSIBLE PERSON
a. REPORT	b. ABSTRACT	c. THIS PAGE	U	6	Nicole Bentley
U/U	U	U			19b. TELEPONE NUMBER (*Include area code*) 518-266-5606

INSTRUCTIONS FOR COMPLETING SF 298

1. REPORT DATE. Full publication date, including day, month, if available. Must cite at lest the year and be Year 2000 compliant, e.g., 30-06-1998; xx-08-1998; xx-xx-1998.

2. REPORT TYPE. State the type of report, such as final, technical, interim, memorandum, master's thesis, progress, quarterly, research, special, group study, etc.

3. DATES COVERED. Indicate the time during which the work was performed and the report was written, e.g., Jun 1997 - Jun 1998; 1-10 Jun 1996; May - Nov 1998; Nov 1998.

4. TITLE. Enter title and subtitle with volume number and part number, if applicable. On classified documents, enter the title classification in parentheses.

5a. CONTRACT NUMBER. Enter all contract numbers as they appear in the report, e.g. F33615-86-C-5169.

5b. GRANT NUMBER. Enter all grant numbers as they appear in the report, e.g. 1F665702D1257.

5c. PROGRAM ELEMENT NUMBER. Enter all program element numbers as they appear in the report, e.g. AFOSR-82-1234.

5d. PROJECT NUMBER. Enter al project numbers as they appear in the report, e.g. 1F665702D1257; ILIR.

5e. TASK NUMBER. Enter all task numbers as they appear in the report, e.g. 05; RF0330201; T4112.

5f. WORK UNIT NUMBER. Enter all work unit numbers as they appear in the report, e.g. 001; AFAPL30480105.

6. AUTHOR(S). Enter name(s) of person(s) responsible for writing the report, performing the research, or credited with the content of the report. The form of entry is the last name, first name, middle initial, and additional qualifiers separated by commas, e.g. Smith, Richard, Jr.

7. PERFORMING ORGANIZATION NAME(S) AND ADDRESS(ES). Self-explanatory.

8. PERFORMING ORGANIZATION REPORT NUMBER. Enter all unique alphanumeric report numbers assigned by the performing organization, e.g. BRL-1234; AFWL-TR-85-4017-Vol-21-PT-2.

9. SPONSORING/MONITORS AGENCY NAME(S) AND ADDRESS(ES). Enter the name and address of the organization(s) financially responsible for and monitoring the work.

10. SPONSOR/MONITOR'S ACRONYM(S). Enter, if available, e.g. BRL, ARDEC, NADC.

11. SPONSOR/MONITOR'S REPORT NUMBER(S). Enter report number as assigned by the sponsoring/ monitoring agency, if available, e.g. BRL-TR-829; -215.

12. DISTRIBUTION/AVAILABILITY STATEMENT. Use agency-mandated availability statements to indicate the public availability or distribution limitations of the report. If additional limitations/restrictions or special markings are indicated, follow agency authorization procedures, e.g. RD/FRD, PROPIN, ITAR, etc. Include copyright information.

13. SUPPLEMENTARY NOTES. Enter information not included elsewhere such as: prepared in cooperation with; translation of; report supersedes; old edition number, etc.

14. ABSTRACT. A brief (approximately 200 words) factual summary of the most significant information.

15. SUBJECT TERMS. Key words or phrases identifying major concepts in the report.

16. SECURITY CLASSIFICATION. Enter security classification in accordance with security classification regulations, e.g. U, C, S, etc. If this form contains classified information, stamp classification level on the top and bottom of this page.

17. LIMITATION OF ABSTRACT. This block must be completed to assign a distribution limitation to the abstract. Enter UU (Unclassified Unlimited) or SAR (Same as Report). An entry in this block is necessary if the abstract is to be limited.

INTRODUCTION

Physical vapor deposition (PVD) is currently being explored as an alternative to electrodeposition for coating the bore of large caliber cannon. PVD is an efficient and environmentally friendly means of producing protective coatings. A number of experimental PVD systems have been developed using cylindrical magnetron sputtering (CMS) to provide a thick metal coating on the bore of cannon. However, adherent, erosion and corrosion resistant coatings are critical to the performance of many weapon systems and the process control parameters that produce the optimal coating properties have not yet been identified. A number of promising coatings have been produced, but a significant number of costly experiments are required before these parameters can be established. Therefore, there is a need for further guidance in selecting the experiments. A model capable of predicting important coating properties such as adhesion, cohesion, density, compositional variation, and uniformity is desirable, but currently not available.

Figure 1 shows the interaction of the components envisioned for a comprehensive model of the CMS system. The DC-discharge is simulated using object-oriented particle-in-cell techniques (OOPIC) [1] to obtain the sputtered particle kinetics and flux distribution. The CMS magnetic field distribution is obtained from a finite element magnetic field model, FEMLAB [2]. The plasma simulation provides the sputtered particle kinetics that is used by a molecular dynamics simulation (XMD) [3] to obtain the cohesive and adhesive properties and phase of the coating material. Finally, A PVD feature scale model (PVDPro) [4] uses the particle kinetics and flux distribution to predict the evolving grain structure, uniformity, compositional variation, and roughness of the coating.

In this investigation, samples were prepared for analysis using a planar target and substrate. PVDPro models cylindrical sputtering chambers with planar targets [5] and substrates, so FEMLAB and XOOPIC simulations were not required to obtain the flux distribution used in simulating grain nucleation and growth.

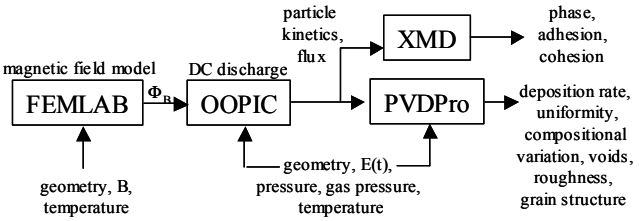

Figure 1. Components of CMS model

BACKGROUND

Physical vapor deposition produces structures that are topologically and morphologically metastable [6]. Metal vapors condense into a fine-grained crystalline form on a cold substrate resulting in evolving structures that are inherently more disordered and less relaxed than those produced by other coating processes. The size, shape, and distribution of these grains affect the material properties and therefore the performance of a coating [7]. The grain structures are a function of self-shadowing, nucleation phenomena, surface diffusion, ion bombardment, and resputtering. They are also a function of process control parameters such as the angular distribution of the incoming flux, deposition geometry, target material, and sputter gas pressure.

Microstructural features can be quantified in terms of self-affine scaling parameters [8,9] to provide details on the intrinsic structure of the coating. The time evolution of these scaling parameters uniquely defines the dynamics of the deposition process. These scaling measures provide insight into the growth processes of coatings and a means of calibrating simulations using experimental data.

APPROACH

The evolution of the grain structure in the simulations and experiments was assumed to adhere to dynamic scaling theory. This approach is used to characterize the evolution of rough surfaces in terms of a growth exponent (α or H), roughness exponent β, and dynamic exponent 1/z [8,9]. Therefore, the coating morphology

was assumed to be a homogenous, self-affine structure with statistical invariance under anisotropic dilations. This assumption applied to the AFM data in view of the scan size used in the measurements, and to the simulated microstructure in the model. The coatings in this study are single-valued surfaces in E^3, which are statistically invariant under transformations of the form:

$$\{x,y,z\} \rightarrow \{\lambda x,\lambda y,\lambda^H z\} \quad (1)$$

where H describes the anisotropic scaling. In a more general case, the y coordinate would have a coefficient λ^K, and in the case of self-similar fractals, H would have a value of 1. The invariance expressed in equation 1 implies that any point on a self-affine surface can be represented in the form $\{\boldsymbol{r},h(\boldsymbol{r})\}$, where the height function $h(\boldsymbol{r})$ is a single valued function of $\boldsymbol{r} \equiv \{x,y\}$.

Anisotropic scaling was measured in terms of the roughness exponent H, parallel correlation length $\xi_{//}(t)$, and the perpendicular correlation length $\xi_{\perp}(t)$. These scaling parameters provide information relating to the intrinsic properties of the surfaces over a range of scales after t minutes of sputtering. The anisotropic scaling described by H applies over a scaling range that is measured in terms of $\xi_{//}(t)$. The parallel correlation length is the distance beyond which there is no correlation in heights between points on the surface. The perpendicular correlation length, $\xi_{\perp}(t)$, characterizes fluctuations in the growth direction. It is related to the RMS surface roughness, $\sigma(t)$, by $\xi_{\perp}(t)= \sqrt{2} * \sigma(t)$. The values of H, $\xi_{//}(t)$, and $\xi_{\perp}(t)$ were determined using a generalized form of the height correlation function [9], $C_h(\boldsymbol{r},t) = \langle [h(\boldsymbol{r}_0+\boldsymbol{r}, t+t_0) - h(\boldsymbol{r}_0,t_0)]^2 \rangle_{t0,\mathbf{r}0}$ where $h(\boldsymbol{r},t)$ is a single valued height of the surface at location $\boldsymbol{r}$ at time t. H is determined from $C_h(\boldsymbol{r},t)$ assuming that the surface is continuous, but not necessarily differentiable [10]. This implies that

$| h(\boldsymbol{r}+\delta,t) - h(\boldsymbol{r},t) | \rightarrow 0$ as $\delta \rightarrow 0$, however, $\lim_{\delta \rightarrow 0} \frac{[h(\boldsymbol{r}+\delta,t)-h(\boldsymbol{r},t)]}{\delta}$ may not exist. Therefore a class of functions is introduced to describe the surface where:
$| h(\boldsymbol{r}+\delta,t) - h(\boldsymbol{r},t) | \propto \delta^H$. The derivative of $h(\boldsymbol{r},t)$ behaves as δ^{H-1} which is finite at H=1. At H = 0, $h(\boldsymbol{r},t)$ is no longer continuous. Therefore, the range $0 < H < 1$ is used to describe a the degree of differentiability of a continuous surface, with increasing H corresponding to a smoother, more Euclidean surface.

Identifying the appropriate scaling region in the $C_h(\boldsymbol{r},t)$ data is critical in obtaining accurate estimates of the scaling parameters. The measured parameters depend on the range of data used to fit the linear region. Therefore, we developed a systematic procedure to determines them by fitting linear and polynomial splines to the height correlation results using the data that minimizes the residuals in the fit [11]. We developed this technique since blind regression fits often result in incorrect values [8].

Correlations between points are time-dependent and generally increase with sputter time. Increasing grain size may be characterized by growth in the lateral ($\xi_{//}(t)$) direction by 1/z. Corresponding changes in the growth direction are described by β. In general, due to anisotropy of the deposition process, $\beta \neq 1/z$. According to dynamic scaling theory, at small sputter times, $\xi_{//}(t)$, and $\xi_{\perp}(t)$ are given by:

$$\xi_{//} \propto t^{1/z} \quad (2)$$

$$\xi_{\perp} \propto t^{\beta} \quad (3)$$

The scaling exponents H, β, and 1/z define a unique *universality class* that is independent of the details of the deposition process. They provide a unique metric for describing the evolving surface structure of the coating and for validating the integrity of the simulation.

A planar magnetron sputtering chamber was employed to sputter deposit niobium on 2 inch silicon wafers for 15, 30, 45, and 75 minutes. The material was sputtered with a 200 Vdc bias voltage at 10 mTorr of argon gas pressure. A Digital Instruments Dimension 3100 Series Scanning Probe Microscope [12] was

used to map surface structures of the niobium coating over a range of scales from 10 nm to 5μm. Lateral resolution was enhanced and lateral forces on the samples eliminated by oscillating the cantilever at its first bending mode resonant frequency using a piezoelectric crystal. In this "Tapping Mode" of operation, the cantilever tip lightly taps the sample during the scan, and contacts the surface at the bottom of its swing [13]. The resonant frequency of the cantilever was 287 KHz and the probe tip was etched silicon having a radius of curvature < 10nm and a sidewall angle of 17°. The AFM images in this investigation are 5 μm square with a 10 nm horizontal resolution and a 0.1 nm vertical resolution.

PVDPro employs Monte Carlo methods to simulate the sputtering of niobium off the target surface based on the process control parameters selected to deposit the niobium samples. Models of the distribution of sputtered material were based on erosion profile measurements of a depleted target obtained from the experimental system. Gas phase collision dynamics were computed with M1 forward scattering [5] in simulating the transport of the sputtered material to the substrate. The distribution of energies and angles of the arriving flux was then used by a feature scale model to simulate nucleation, self-shadowing, and surface diffusion on the film and substrate. Particles that adsorb on the surface migrate over a given diffusion length before being incorporated into the film. The final position of the particle is the site within the diffusion length, L, which minimizes the surface free energy. The activation energies for surface diffusion on the substrate and film are not well known for most materials, therefore the temperature dependence is not explicitly modeled.

The feature scale simulation of grain evolution is particle based, so surface wetting cannot be expressed in terms of a wetting angle as in continuum models. It is, instead, expressed in terms of a percentage, with 100% corresponding to perfect wetting.

The simulation parameters in this study spanned the entire available range in PVDPro. The selected values for surface wetting were 20%, 50%, and 100%. The substrate and film diffusion lengths were both set equal to 0.015 μm, 0.026 μm, and 0.036 μm. The topology of 0.10 μm, 0.20 μm, 0.40 μm, and 0.80 μm thick coatings were extracted for analysis. This corresponds to t = 0.14, 0.45, 0.55, and 0.71 minutes of simulated sputtering for the process control parameters selected in the model. The topology of the grain structure was then extracted and quantified in terms of self-affine scaling exponents. The results were then compared to experimental values to determine the optimal parameters to use in the simulation.

RESULTS

Figure 2 shows AFM images of the niobium coating after t =15, 30, 60, and 75 minutes of sputtering and figure 3 shows the corresponding $C_h(\boldsymbol{r},t)$. The $C_h(\boldsymbol{r},t)$ data in figure 3 indicate that the grain structure of the niobium coating is essentially Euclidian (0.88), with the grain size ($2*\xi_{//}$) increasing from 188 nm to 368 nm. The values of grain size were validated with micrographs of the coatings. Figure 4 gives the time dependence of $\xi_{//}(t)$ and $\xi_{\perp}(t)$, assuming that the evolving grain size and roughness are consistent with dynamic scaling theory. The value of β was determined to be 0.27 and 1/z = 0.37 using all of the data for the fit. These results agree well with published results for sputtered deposited coatings [14].

Figure 5 shows the grain profiles for a simulated 0.80 μm niobium coating with 20% surface wetting with L = 0.015μm & 0.036 μm. The particles in PVDPro represent clusters of atoms with similar dynamics. Particle size is user-defined, with higher resolution simulations quickly exhausting computational resources. However, the smallest available particle size, 5.1 nm, was selected based on the measured value of $\xi_{\perp}(15)$ = 37 nm for the niobium samples. This imposed computational constraints on the size of the simulations for this study. Simulations were limited to a maximum coating thickness of 0.80 μm.

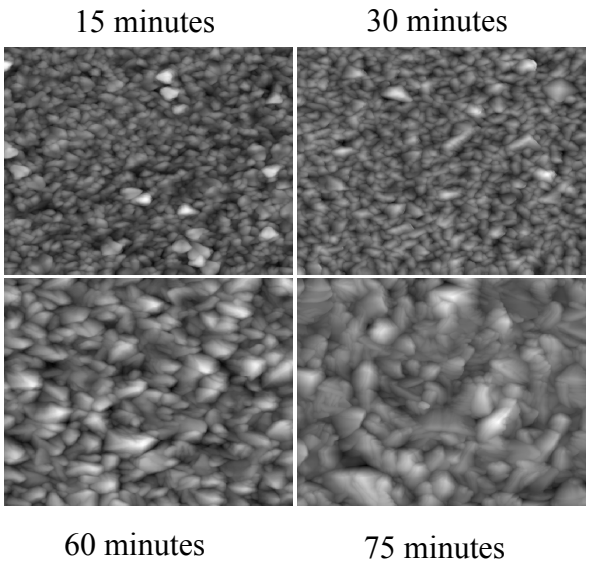

Figure 2. 5 µm AFM scans of niobium after t = 15, 30, 60, and 75 minutes of sputtering.

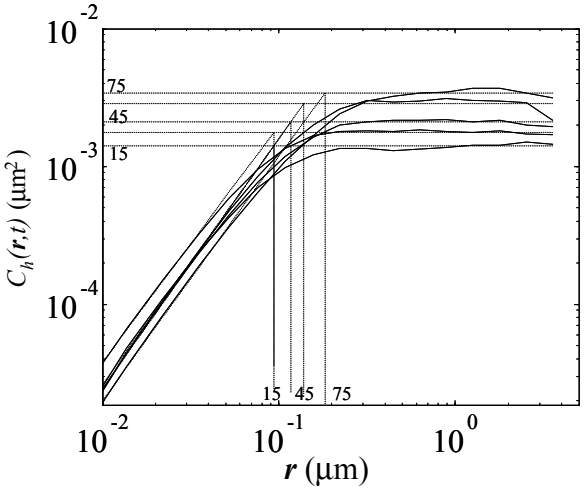

Figure 3. $C_h(r,t)$ for sputtered niobium after t = 15, 30, 45, 60 and 75 minutes of sputtering.

In all of the simulations, increasing L increased the density and reduced the complexity of the grain microstructure. This smoother, more Euclidean structure is reflected in the increasing values of H as given in Table 1. The table shows H, grain size ($2*\xi_{//}$), and $\xi_{\perp}$ for a 0.80 µm simulated coating with 20%, 50%, and 100% surface wetting and 0.015 µm, 0.026 µm, and 0.036 µm diffusion lengths. H correlates directly with L and increases from a mean value of 0.54 ± 0.01 to 0.64 ± 0.02. $\xi_{\perp}$ increases marginally with L, from a mean value of 0.033 ± 0.001 to 0.036 ± 0.002 µm. The effect of surface wetting on the analysis is not apparent.

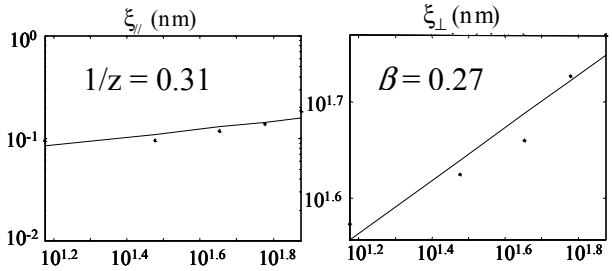

Figure 4. $\xi_{//}$ (t) and $\xi_{\perp}$(t) for sputtered niobium

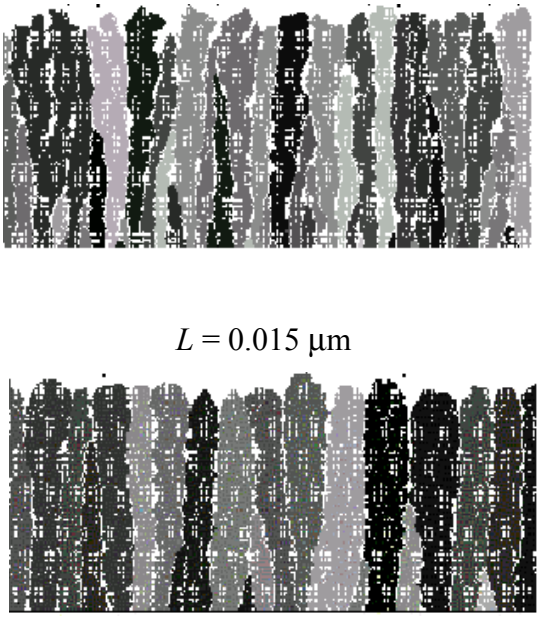

Figure 5. PVDPro feature scale simulation of a 0.80 µm coating on a 2 µm substrate with L = 0.015 and 0.036 µm.

wetting %	L (μm)	H	$\xi_{//}$ (μm)	$\xi_{\perp}$ (μm)
20	0.015	0.56	0.039	0.034
20	0.026	0.67	0.036	0.037
20	0.036	0.65	0.038	0.038
50	0.015	0.53	0.034	0.032
50	0.026	0.57	0.034	0.031
50	0.036	0.61	0.034	0.033
100	0.015	0.54	0.036	0.033
100	0.026	0.58	0.037	0.032
100	0.036	0.66	0.038	0.036

Table 1. Scaling parameters for simulated 0.80 μm coating with different wetting % and diffusion lengths.

The scaling exponents of the niobium coating were used as a guide to determine the optimal parameters to use in the model. β and 1/z were used to predict the grain structure at the small sputtering times that constrain the model. The grain structure of the niobium coating is essentially Euclidean, so only simulations with $L = 0.036$ μm were considered. The scaling parameters were determined for 0.10 μm, 0.20 μm, 0.4 μm, and 0.80 μm coatings using 20% and 100% surface wetting. The effect of the finite AFM probe tip radius was also incorporated in the analysis of the grain profile. ***h(r)*** was limited by any interference detected between the simulated surface and a probe having a 10nm radius of curvature and 17° sidewall angle. This resulted in an effective grain structure with $H = 0.81 \pm 0.01$, which is more consistent with the observed data.

The effect of surface wetting is reflected in the intergranular porosity of the microstructure. However, the results of height correlation analysis shown in Table 2 suggest that surface wetting does not affect the evolution of surface topology. Therefore, the results of the 20% and 100% wetting simulations were averaged to compute the dynamic scaling parameters. This resulted in a roughness exponent (β) of 0.39 and dynamic exponent (1/z) of 0.29 using all points in the fit.

Figures 6 and 7 shows the simulation results and the predicted values for $\xi_{//}(t)$ and $\xi_{\perp}(t)$ based on analysis of the AFM data. The figures indicate that the evolution of the observed data and the simulated microstructure are consistent with the assumptions of dynamic scaling theory. The agreement between scaling exponents is reasonable given that only H was used to select parameters used in the model.

wetting %	coating thickness (μm)	H	$\xi_{//}(t)$ (μm)	$\xi_{\perp}(t)$, (μm)
20	0.10	0.81	0.022	0.014
20	0.20	0.80	0.026	0.018
20	0.40	0.82	0.027	0.020
20	0.80	0.82	0.038	0.030
100	0.10	0.79	0.021	0.012
100	0.20	0.80	0.024	0.017
100	0.40	0.82	0.030	0.023
100	0.80	0.81	0.039	0.030

Table 2. Scaling parameters for evolving coating with $L = 0.036$ μm, and 20% and 100% surface wetting

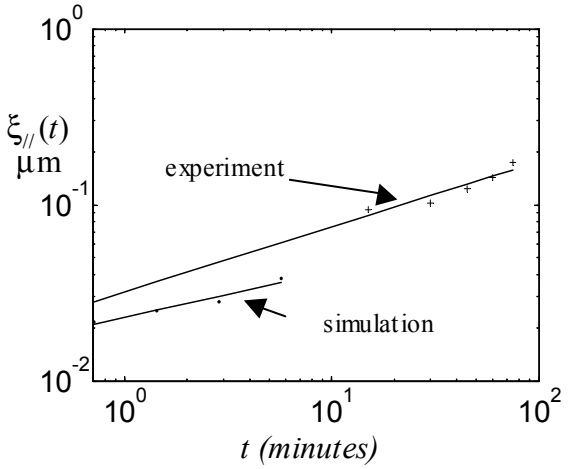

Figure 6. $\xi_{//}(t)$ for simulated and experimental grain profiles.

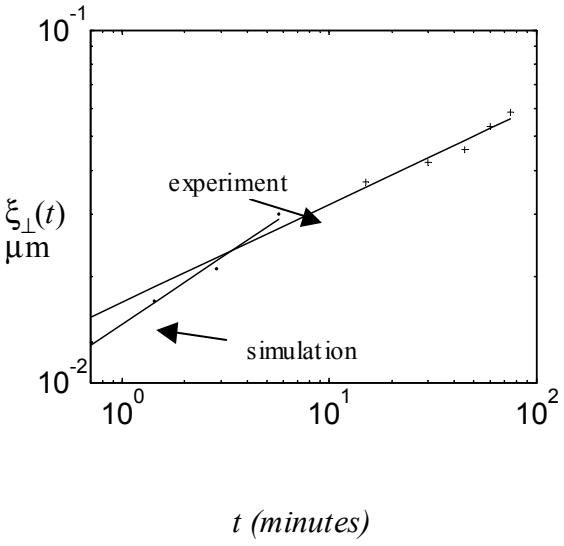

Figure 7. $\xi_{\perp}(t)$ for simulated and experimental grain profiles.

CONCLUSIONS

1. The surface morphologies of the simulated and experimental coatings analyzed in this study are consistent with those of self-affine surface fractals. In most cases, a single exponent, H, characterizes the scaling. The observed grain structure of the observed and sputtered deposited niobium is nearly Euclidean.

2. The scaling parameter H, and dynamic scaling parameters β, and 1/z, provide a useful metric to quantify the evolution of grain structure, size, and surface roughness. The metric can be used to compare simulation results with experimental data and provide a means of optimizing simulation parameters using experimental measurements.

3. Identifying the appropriate scaling region in $C_h(\boldsymbol{r},t)$ data is critical when measuring subtle changes in the scaling parameters of real data. Fitting linear and polynomial splines to $C_h(\boldsymbol{r},t)$ data provides a systematic approach for measuring the scaling parameters.

4. The simulation of the evolving grain structure of sputter deposited niobium is consistent with observed changes in grain structure, and both the model and experiment are consistent with dynamic scaling theory.

REFERENCES

[1] Verboncoeur, J.P.; A.B. Langdon; N.T. Gladd. 1995. "An Object-Oriented Electromagnetic PIC Code", *Comp. Phys. Comm.*, No. 87, May:11, 199-211.
[2] COMSOL, Inc., *FEMLAB*, 8 New England Executive Park, Burlington, MA 01803, USA
[3] University of Connecticut, *XMD*, Storrs, Ct
[4] Reaction Design. 2001. *PVDPro, Version 3.2*, 6440 Lusk Boulevard, Suite D-209. San Diego, CA, USA (2001)
[5] Reaction Design. 2000. *PVDPro Version 3.2 Users Guide*, San Diego, CA.
[6]Turnbull, D. 1981. Metastable Structures in Metallurgy, *Metallurgical Transactions A*, No. 12 A, pp. 695-708.
[7] Thorton, J.A.. 1986. "The Microstructure of Sputter Deposited Coatings", *Journal of Vacuum Science and Technology*, No. A4(6), Nov/Dec
[8] Barabasi, A.L. and H.E. Stanley H.E. 1995. *Fractal Concepts in Surface Growth*, Cambridge University Press
[9] Gouyet, J.; M. Rosso; B. Sapoval. 1991. *Fractals and Disordered Systems*, eds. A. Bunde and S. Havlin, Springer, Berlin, 229-234.
[10] Korvin, G. 1992. *Fractal Models in the Earth Sciences*, Elsevier Science Publishers.
[11] Johnson, M.A. 2000. "Measuring Dynamic Scaling Exponents in Evolving Structures", *Proceedings of the Systemics, Cybernetics, and Informatics Conference*, (Orlando Fl, July 23-26), SCI, No 5, 112-116.
[12] Digital Instruments Corporation, 112 Robin Hill Road, Santa Barbara CA, USA
[13] Digital Instruments Corporation. 1998. *Scanning Probe Microscopy Training Notebook*, Santa Barbara, CA.
[14] Miller, D.J.; K.E. Gray; R.T. Kampwirth; J.M. Murduck. 1992. "Studies of Growth Instabilities and Roughening in Sputtered NbN Films Using a Multilayer Decoration Technique", *Europhys. Lett*. No. 19, 27-32.